ACS Sustainable Chemistry & Engineering

Research Article

pubs.acs.org/journal/ascecg

Chemically Amplified Dehydration of Thin Oxide Films

Jeremy T. Anderson,[†] Wei Wang,[‡] Kai Jiang,[†] Torgny Gustafsson,[§] Can Xu,[§] Eric L. Gafunkel,[⊥] and Douglas A. Keszler*[,‡]

[†]Inpria Corporation, 2001 Monroe Avenue, Corvallis, Oregon 97330, United States

[‡]Department of Chemistry, Oregon State University, 153 Gilbert Hall, Corvallis, Oregon 97331-4003, United States

[§]Department of Physics and Astronomy, Rutgers University, Piscataway, New Jersey 08854, United States

[⊥]Department of Chemistry and Chemical Biology, Rutgers University, Piscataway, New Jersey 08854, United States

Supporting Information

ABSTRACT: The hydrous material $Al(PO_4)_{0.6}O_{0.6}{\cdot}zH_2O$ (AlPO) is studied in thin-film form to determine whether bulk diffusion or near-surface densification controls thermal dehydration. From X-ray reflectivity measurements, a dense surface crust is found to form on heating AlPO films. Capacitance−voltage measurements reveal the presence of mobile protons associated with trapped −OH and H_2O in the films. Deposition of a thin solution-processed HfO_2 top coat on the AlPO film lowers the dehydration temperature by 250 °C. Characterization of the AlPO/HfO_2 interface by medium energy ion scattering and transmission electron microscopy reveals little interdiffusion between the layers. The top coat affects densification of the near-surface region of the AlPO film, thereby amplifying water loss at low temperatures.

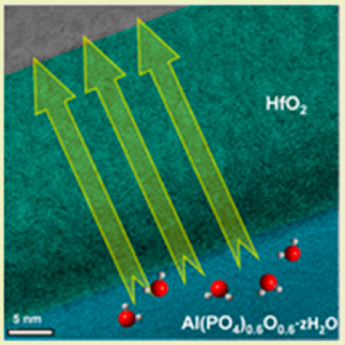

KEYWORDS: *Oxide films, Aqueous processing, Electronic materials*

INTRODUCTION

We introduce a new chemical approach to remove water from aqueous-processed thin inorganic oxide films. Nature's solvent, water, has long been considered the preferred medium for depositing oxide coatings, yet aqueous deposition finds remarkably little use compared with vacuum methods. This limited practice is generally attributed to compromised film function, such function being commonly traced to poor morphology, defects, low density, and retained solvent. In practice, the expulsion of starting ligands from a precursor and associated solvent loss lead to film surface roughness, bulk inhomogeneities, and defect trap states. Supplying energy to improve these characteristics, whether by thermal, optical, or microwave methods, can lead to unwanted interdiffusion and reaction between adjacent layers; moreover, these methods rarely improve the quality of a film. A chemical strategy offering reduced processing temperatures to effectively dehydrate and dry films provides a unique approach to conserving energy in film deposition. Accordingly, we have modified the surface of a wet oxide by simply adding a surface film of another material. In this way, dehydration of the bulk film is dictated by the new interfaces created, amplifying physical treatments that promote and preserve water loss at reduced processing temperatures. This boost in dehydration can dramatically improve function, as we will demonstrate by the enhanced performance of thin-film transistors.

In our strategy, we select chemically complementary layers such that the top layer amplifies dehydration of the oxide layer beneath. Specifically, in this study we apply a very thin top coat of solution-deposited HfO_2 to a hydrated aluminum oxide phosphate (AlPO) film. Relative to the bare AlPO film, the top coat is found to reduce the effective dehydration temperature of the underlying AlPO film by approximately 250 °C. By fabricating and testing thin-film transistors with AlPO gate insulators with and without the top coat at the same temperature, we find the insulator with the top coat produces a much more stable device. This stability is directly correlated to material interfaces and water content measured via several high-resolution analytical techniques.

The chemical trends and principles of dehydration temperatures for inorganic hydroxides and hydrates have not been established. In addition, the significance of residual water in oxide materials is rarely appreciated; a multidisciplinary perspective is necessary to express the nature of this problem and the basis for our approach. Oxide thin films, whether vapor- or solution-deposited, often contain hydrogen in the form of hydroxide or water. Such incidental hydrogen is known to compromise the performance of thin-film electronic devices. In dielectrics, this hydration can give rise to defect trap states and mobile charge, which compromises breakdown field strength, creates device instabilities, and results in poor performance.[1−3] Hydrogen and water in these thin films is most commonly eliminated by heating via optical, microwave, or conventional thermal methods. Relatively limited information is available

Received: December 19, 2014
Revised: February 27, 2015
Published: April 30, 2015

DOI: 10.1021/sc500824a
ACS Sustainable Chem. Eng. 2015, 3, 1081−1085

concerning chemical routes that might facilitate dehydration of thin oxide films, and thereby amplify the effects of radiation and thermal processing. Conversely, the geology and geochemistry communities have extensively studied water migration in hydrous oxide minerals, as water plays a crucial role in several geological phenomena.[4−6] Mineral dehydration has been investigated by both experimental and computational methods.[5,7,8] Empirically, small-particle powders with high surface areas are found to dehydrate faster than large-particle powders of the same material.[9] It is generally assumed that bulk diffusion processes of hydrogen (either via −OH or H_2O) control the dehydration times across a very substantial temperature range.[10,11] Although this explanation correlates small particles to short diffusion lengths, the behavior could also be attributed to near surface rearrangement and densification. In that case, diffusion of water through the surface may be play a dominate role in the dehydration process. In turn, an interface may be manipulated by a relatively small compositional change, such as a very thin top coat.

RESULTS AND DISCUSSION

We illustrate this new strategy with the thin-film dielectric material $Al(PO_4)_{0.6}O_{0.6}{\cdot}zH_2O$ commonly known as "AlPO". As an amorphous oxide insulator, AlPO has been incorporated into a number of high-performance thin-film transistors (TFTs) via aqueous processing.[12,13] We have found that AlPO films must be heated above 600 °C to force dehydration and eliminate the mobile species that cause unstable TFT operation. By applying a very thin layer of HfO_2 from an aqueous precursor[14] to the AlPO film, we demonstrate an effective materials combination that decreases the dehydration temperature of AlPO and dramatically improves dielectric performance.

A capacitance−voltage (C−V) measurement of a metal−insulator−metal (MIM) test structure reveals the level of mobile charge in an insulating oxide film (Figure 1a). The mobile charges in an oxide film, such as AlPO, move in response to the external field, contributing to the capacitance and hysteresis in the C−V curve. By using pre-DC-bias capacitance (C_0) as reference, the relative capacitance change ($C - C_0$) is determined as a function of applied field (Figure 1b). A device with an AlPO insulator (200 nm thick), previously heated for 1 h at 350 °C, exhibits an increase of 22 000 ppm in relative capacitance on sweeping from 0 to ±1.5 MV/cm applied DC field. As shown by the dashed arrow in Figure 1b, the zero-bias capacitance increases by approximately 7000 ppm following the positive and negative voltage sweeps, demonstrating pronounced hysteresis. This hysteresis indicates the presence of sluggish mobile charges in the AlPO layer, most likely the result of residual protons.[12] If the test structure is made with a thin HfO_2 top coat (about 20 nm) and annealed at the same temperature, the relative capacitance changes by only 5000 ppm with zero-bias hysteresis <100 ppm (Figure 1b). Hence, the relative transient capacitance decreases by a factor of 70.

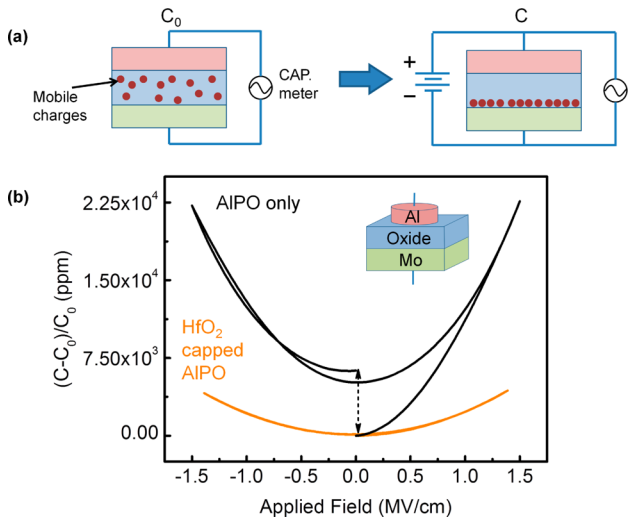

Figure 1. (a) C−V measurement setup for an MIM capacitor; (b) one sweep cycle of MIM capacitors with an AlPO insulator (black) and a HfO_2−AlPO insulator (orange). Both insulating oxide films were annealed at 350 °C for 1 h.

The 20 nm HfO_2 layer is found to effectively promote the removal of mobile charge from the oxide stack. Thinner layers also facilitate the dehydration, with at least ∼8−10 nm of HfO_2 required to achieve the same level of electrical performance. Moreover, as shown in Figure S1 of the Supporting Information, the dehydration enhancement with the HfO_2 layer occurs after only a 5 min anneal at 350 °C. AlPO-only films require annealing above 500 °C for 1 h to reach a similar level of dehydration, though the transient electrical behavior is less ideal. To appreciate how the mobile charge and its suppression translate to a switching device, discrete *n*-type TFTs were fabricated in an identical manner by using bare AlPO or HfO_2-coated AlPO gate insulators (Figure S2 of the Supporting Information). Devices were stressed with the negative pole adjacent to the semiconductor with a field of 1.5 MV/cm across the dielectric at T = 60 °C for 3000 s. Following stress, AlPO-only devices could no longer be switched off, even when applying an opposite field of 2 MV/cm. In contrast, the HfO_2-coated AlPO devices require a poststress compensation field of only ∼0.1 MV/cm to switch them off. Clearly, differences in the dielectric mobile charges dominate the ability to operate even single transistors; these effects are only amplified in device arrays and integrated circuits.

Physical and chemical examination of the film structure and HfO_2/AlPO interface was initiated with medium energy ion scattering (MEIS). As a high-resolution variant of Rutherford backscattering spectroscopy for ultrathin films[15] (Figure 2a), it has been used in this study to determine the total areal density (atoms/cm^2) of Hf in the HfO_2/AlPO/SiO_2 structure and a HfO_2/SiO_2 control and to measure compositional depth

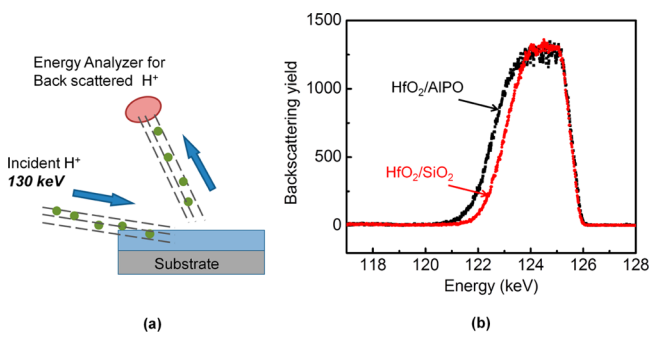

Figure 2. (a) MEIS scattering geometry (b) MEIS spectra of HfO_2 thin films on Si and AlPO.

DOI: 10.1021/sc500824a
ACS Sustainable Chem. Eng. 2015, 3, 1081−1085

profiles. Importantly, these measurements reveal whether any significant interdiffusion occurs at the HfO_2/AlPO interface. For the HfO_2/AlPO structure (MEIS spectrum Figure 2b), we determine that the HfO_2 film has an areal density of 1.36×10^{16} Hf atoms/cm^2, a thickness of 6.0 nm (assuming a density of 8.5 g/cm^3), and uniform depth profile. The low-energy portions of the ion spectra yield information about the uniformity of the film. If the film is rough at the outer surface or inner interface, or if there is interdiffusion, then the low energy tail will broaden, sometimes significantly. Because the HfO_2/SiO_2 and HfO_2/Si interfaces produced by ALD and solution deposition of HfO_2 are known to be rather sharp, we used a solution-deposited HfO_2 on SiO_2/Si to compare with the HfO_2/AlPO interface. As there is no noticeable broadening of the tail of the Hf peak in the HfO_2/AlPO structure (Figure 2b) relative to that in the HfO_2/SiO_2 structure, we find no evidence for interdiffusion between the HfO_2 and AlPO layers beyond perhaps a few angstroms.

The MEIS studies have been complemented with transmission electron microscopy (TEM) imaging of the HfO_2/AlPO structure (Figure 3). The high-resolution TEM image

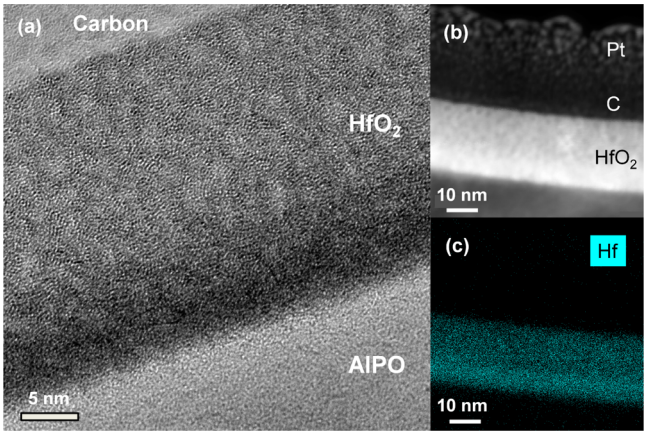

Figure 3. (a) High resolution TEM image of the HfO_2–AlPO interface region after annealing at 350 °C for 1 h; (b) Z-contrast STEM image showing the interface region; (c) ChemiSTEM Hf elemental mapping at the position of image (b).

(Figure 3a), Z-contrast scanning transmission electron microscopy (STEM) image (Figure 3b), and ChemiSTEM elemental mapping (Figure 3c) all indicate a sharp interface between HfO_2 and AlPO consistent with the MEIS results. Interestingly, in all images a significant change in contrast is observed in the HfO_2 layer from top to bottom. As seen in Figure 3c, this contrast is consistent with 10–12 nm of high-density HfO_2 directly on top of the AlPO (which is comparable to the minimum thickness required for stable TFT operation). A less dense, likely porous structure exists above this dense region. This same HfO_2 structure is also observed after a 5 min anneal at 350 °C (Figure S3 of the Supporting Information).

To quantify the hydrogen concentration and estimate the level of dehydration in the AlPO layer, elastic recoil detection analysis (ERDA, also known as hydrogen forward scattering when analyzing hydrogen) was performed on both AlPO and HfO_2/AlPO samples. In ERDA, a high-energy He^{2+} ion beam is directed onto a material at a shallow angle (Figure 4a), causing forward scattering of hydrogen in the film. The hydrogen atomic percentages, determined for the AlPO and HfO_2/AlPO films after different annealing treatments, are shown in Figure

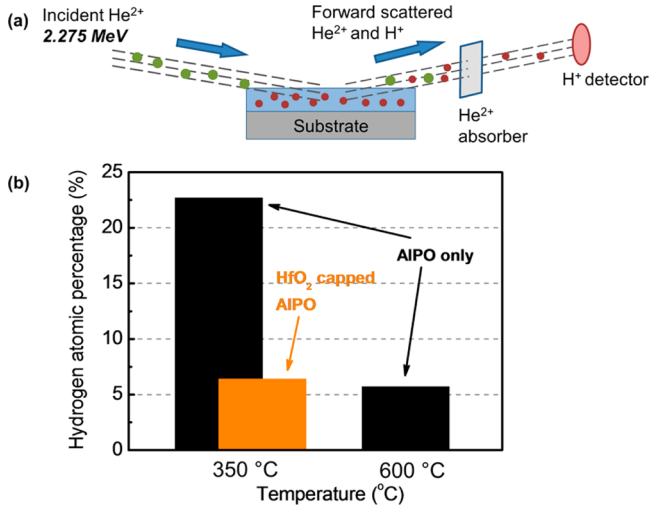

Figure 4. (a) ERDA geometry; (b) hydrogen atomic percentages (relative to atomic total) in AlPO films annealed at 350 and 600 °C (black), and HfO_2-capped AlPO heat to 350 °C (orange). All anneals are 1 h.

4b. A bare AlPO film (200 nm) contains 23 at. % hydrogen (1.5 H per Al) after a 1 h anneal at 350 °C. Annealing at 600 °C for 1 h decreases the hydrogen content to 5.7 at. %. When a HfO_2 top coat (about 20 nm) is present, the total hydrogen content in the entire stack drops to 6.3 at. % (0.35 H per Al) after a 350 °C anneal, which is comparable to the bare AlPO layer annealed at 600 °C. Although there is still hydrogen in the HfO_2/AlPO stack, it is likely to be tightly bound within the amorphous network such that it is electrically inactive in devices. Fourier transform infrared spectroscopy (FTIR) of HfO_2-capped-AlPO and AlPO-only dielectrics annealed at 350 °C for 1 h (Figure S4 of the Supporting Information) also show a significant decrease in the −OH stretching signal after applying the HfO_2 surface layer. This is consistent with the decreased water content in the layers.

To construct a physicochemical model of the amplified dehydration, it is beneficial to first consider the characteristics of individual AlPO and HfO_2 films. AlPO is amorphous to temperatures >1000 °C. Because it retains mobile water at moderate temperatures, we examined the vertical density profile of selected films via X-ray reflectivity (XRR). Single-coat films with thicknesses near 6.5, 13, and 20 nm and a triple-coat film with thickness near 18.7 nm were produced by annealing at 350 °C. For each single-coat film, the XRR data (Figures S5–S7 of the Supporting Information) could only be modeled with a bilayer structure, i.e., a thick bottom layer with a density of 2.5–2.6 g/cm^3 and a 0.8–1.4 nm thin top layer with a density >3 g/cm^3. Similarly, the XRR data (Figure S8 of the Supporting Information) for the multiple-coat film could only be modeled with a bilayer structure for each deposition step. In each case, a "crust" of ~0.8–1.5 nm thickness forms at the AlPO/air interface. We propose that the AlPO-only films form a "crust" in the initial stages of dehydration, which could inhibit the migration of additional water through the surface region of the film. Solution-deposited HfO_2 typically crystallizes at temperatures below 500 °C.[14] The material is essentially dehydrated by 400 °C[14] concurrent with the formation of crystalline nuclei. In contrast to the observations on AlPO, a thermally induced high-density surface "crust" has not been observed in the HfO_2 film.

DOI: 10.1021/sc500824a
ACS Sustainable Chem. Eng. 2015, 3, 1081–1085

When HfO_2 is applied from a solution precursor to AlPO films and annealed, amplified thermal dehydration of the AlPO layer cannot be attributed to interdiffusion of materials, according to MEIS data and elemental mapping. In the AlPO/HfO_2 bilayer, it is likely that contact with HfO_2 prevents this localized densification and AlPO "crust" formation, the interface affording a smooth connection between layers and a continuous path for water migration. The top porous region of HfO_2 may also contribute by drawing water from the denser interface, but the top-layer morphology has not been thoroughly studied across a wide range of HfO_2 thicknesses, including the key range of ∼8−12 nm, which may coincide with surface crystallite formation. It is noteworthy that the AlPO layer remains homogeneous, as indicated by TEM images and by dielectric integrity. The film also largely retains its thickness on dehydration (Table S1 of the Supporting Information), meaning its atomic number density decreases uniformly. We conclude that AlPO-only dehydration is not dictated by simple bulk diffusion, but is strongly influenced by surface traits.

A daily-life example provides an analogy of how surface and bulk materials properties and their water response can differ and change with temperature. Developed thousands of years ago, bread baking is an essential food production activity, and for many, is symbolic of a healthy life. Through the baking process, the crust encasing a loaf of bread can be dry and crisp, while the center remains moist and soft. Although the complex chemical changes that occur during bread baking are still being actively investigated, it is well-known that the nature of crust formation significantly affects water loss during baking and overall bread quality.[16,17] So, it is not surprising that baking techniques such as the introduction of steam can be used to control crust formation and bread texture.[16−19] Interestingly, this same "steam baking" method has been directly applied to the dehydration and formation of oxide semiconductors.[20] In our work, depositing the surface material HfO_2 inhibits "crust" formation, thereby promoting the effects of dehydration.

In this contribution, we studied dehydration in a new way. We propose upon heating that the near-surface region of a film may chemically and structurally rearrange more quickly than bulk regions, thereby dictating the rate of water transport across the film−air interface. For example, if heating creates a preferentially dense surface layer, it can act as a barrier to dehydration and rehydration. High temperatures are then required to promote diffusion and water movement across a dense surface "crust". We hypothesize that the drying of a material can be affected by application of a thin layer of a top coat that controls the formation of this crust. In particular, we have studied the dehydration of AlPO thin films with and without a thin HfO_2 capping layer. On the basis of chemical compatibility and water mobility, the HfO_2 layer is found to enhance the effects of dehydration. The observed effect does not depend on phase mixing or interdiffusion. Yet, it is sufficiently powerful to render a mild 350 °C anneal equivalent to that of a 600 °C anneal. The HfO_2-coated AlPO structure, which expels more water and consequently reduces mobile charge, is also a more ideal dielectric than AlPO alone. Indeed, the dielectric performance is unprecedented for a solution-deposited film at such low temperatures. Overall, the results illuminate the need to examine the near-surface properties of solid materials in the context of dehydration and hydration processes. They also inform new strategies for exploring and designing materials and methods for broader application of chemically amplified dehydration. The results can be generally applied to mass transport in both directions across any materials interface.

EXPERIMENTAL SECTION

Solution Precursor Synthesis and Thin-Film Deposition. The AlPO (nitrate based) solution at 0.9 M and the peroxide-containing HfO_2 precursor at 0.2 M were synthesized following the procedure described in refs 12 and 14, respectively. The aluminum to phosphorus ratio in the AlPO solution is 5:3.

Prior to thin-film deposition, all substrates were treated with a thorough Millipore water rinse followed by a low-energy O_2 plasma ash to create a clean and hydrophilic surface. Films were deposited by spin coating the aqueous precursors at 3000 rpm for 30 s and then immediately cured on a hot plate at 230 °C for 1 min. This step was repeated until the desired layer or stack structure was obtained. A 0.9 M AlPO precursor produced 90−100 nm of baked film (depending on spin velocity), whereas a 0.2 M HfO_2 precursor produced 7−8 nm. Films were further annealed in air at 350−600 °C for 5−60 min.

Electrical Device Characterization. Corning 1737 glass with 200 nm sputtered Mo was used as the substrate for fabricating MIM capacitors. AlPO films (∼180−200 nm) were deposited by spin coating with and without an HfO_2 top layer and then annealed. Circular Al top contacts (200 nm thick, 0.011 cm^2) were thermally evaporated through a shadow mask. Capacitance−voltage ($C-V$) measurements were made with an Agilent E4980A LCR meter (VAC = 100 mV at 1 kHz). The DC voltage range was selected according to the oxide thickness to obtain a consistent electric-field strength (1.5 MV/cm) across the oxide layer. The change of capacitance under applied DC bias and the resulting hysteresis were monitored. $C-V$ measurement results could be reproduced after a suitable settling time, so results were not a product of labile fabrication defects. Also, field sweep cycles beginning in the negative or positive directions produced mirror-image responses.

Bottom-gate thin-film transistors were fabricated to assess the device bias stability associated with by the gate dielectrics. ∼200 nm of AlPO thin film or HfO_2-capped-AlPO stack was deposited onto a Mo-coated glass substrate as the gate dielectric layer. ∼30 nm IGZO *n*-type channel layer was deposited via solution processing onto both dielectrics. The channel layer and source/drain contact were patterned by photolithography to define the W/L ratio of 5 (channel width = 500 μm, channel length = 100 μm). All solution deposited layers were annealed at 350 °C for 1 h after the deposition. ∼200 nm Al source and drain contacts were deposited by thermal evaporation via shadow mask. The transistors were characterized on a heating stage in a dark box with a Hewlett-Packard 4156C precision semiconductor parameter analyzer. Transfer curves were measured with V_D (drain voltage) = 0.1 V while sweeping the gate voltage (V_G) from −10 to +30 V. The source contact was grounded during measurement. The bias-temperature stress testing was done by applying V_G = 30 V to the devices for 3000 s at room temperature and 60 °C. The transfer behavior was measured before and after applying the bias and temperature stress.

Thin-Film Characterization. A HfO_2−AlPO stack containing ∼24 nm HfO_2 and ∼180 nm AlPO was studied by TEM and STEM. Sample preparation was done by using an FEI Helios Dual−Beam FIB. A platinum layer was deposited during the preparation to protect the thin film from electron-beam damage. A carbon layer was thermally evaporated onto films before the deposition of the Pt layer to provide imaging contrast. *p*-Si was used as the substrate for all TEM studies. High resolution transmission electron microscopy (HRTEM) images and selected area electron diffraction (SAED) images were taken on an FEI Titan 80-300 transmission electron microscope equipped with a 300 kV electron beam. STEM and ChemiSTEM elemental analyses were done on an FEI Titan 80−200 transmission electron microscope equipped with a 200 kV electron beam.

A HfO_2−AlPO stack containing a single layer of HfO_2 and ∼20 nm AlPO was studied by medium energy ion scattering. The measurement was performed at the Rutgers ion scattering facility by using 135 keV protons. Additional details about MEIS methods can be found in ref

DOI: 10.1021/sc500824a
ACS Sustainable Chem. Eng. 2015, 3, 1081−1085

15. Hydrogen forward scattering (HFS) measurements (elastic recoil detection analysis for hydrogen) were done by Evans Analytical Group on both AlPO thin film and HfO_2−AlPO stacks (sample details are described in the Supporting Information). All films were deposited on *p*-Si substrates for the HFS measurements. Hydrogen content in the AlPO layer was analyzed by modeling the scattering spectra in each sample, which is a direct indication of the residual water level in AlPO.

■ ASSOCIATED CONTENT

Supporting Information

CV, TFT, FTIR, XRR, ellipsometry, and hydrogen forward scatting data, TEM image. The Supporting Information is available free of charge on the ACS Publications website at DOI: 10.1021/sc500824a.

■ AUTHOR INFORMATION

Corresponding Author

*E-mail: douglas.keszler@oregonstate.edu (D.A.K).

Author Contributions

J.T.A. and W.W. contributed equally to the paper.

Notes

The authors declare the following competing financial interest(s): D.A.K. has a financial interest in Inpria Corporation.

■ ACKNOWLEDGMENTS

This material is based upon work in the Center for Sustainable Materials Chemistry, which is supported by the U.S. National Science Foundation under grant number CHE-1102637. W.W. acknowledges support from The Ben and Elaine Whiteley Endowment for Materials Research. T.G. and C.X. acknowledge funding from the U.S. National Science Foundation under grant number DMR-1126468. Sujing Xie and Richard Oleksak contributed to acquisition of the TEM data.

■ REFERENCES

(1) Ip, K.; Overberg, M. E.; Heo, Y. W.; Norton, D. P.; Pearton, S. J.; Stutz, C. E.; Luo, B.; Ren, F.; Look, D. C.; Zavada, J. M. Hydrogen incorporation and diffusivity in plasma-exposed bulk ZnO. *Appl. Phys. Lett.* **2003**, *82*, 385−387.

(2) Fleetwood, D. M.; Warren, W. L.; Schwank, R.; Winokur, P. S.; Shaneyfelt, M. R.; Riewe, L. C. Effects of interface traps and border traps on MOS postirradiation annealing response. *IEEE Trans. Nucl. Sci.* **1995**, *42*, 1698−1707.

(3) Onishi, K.; Kang, C. S.; Cho, H.-J.; Kim, Y. H.; Nieh, R. E.; Jeong, H.; Krishnan, S. A.; Akbar, M. S.; Lee, J. C. Bias-temperature instabilities of polysilicon gate HfO_2 MOSFETs. *IEEE Trans. Electron Devices* **2003**, *50*, 1517−1524.

(4) Harlov, D. E.; Johansson, L.; Van Den Kerkhof, A.; Forster, H. J. The role of advective fluid flow and diffusion during localized, solid-state dehydration: Söndrum stenhuggeriet, Halmstad, SW Sweden. *J. Petrol.* **2006**, *47*, 3−33.

(5) Bray, H. J.; Redfern, S. A. T. Kinetics of dehydration of Ca-montmorillonite. *Phys. Chem. Miner.* **1999**, *26*, 591−600.

(6) Cheng, H.; Liu, Q.; Xiaonan, C.; Zhang, Q.; Zhang, Z.; Frost, R. L. Mechanism of dehydroxylation temperature decrease and high temperature phase transition of coal-bearing strata kaolinite intercalated by potassium acetate. *J. Colloid Interface Sci.* **2012**, *376*, 47−56.

(7) Wright, K. Atomistic models of OH defects in nominally anhydrous minerals. *Rev. Mineral. Geochim.* **2006**, *62*, 67−83.

(8) Madejová, J. FTIR techniques in clay mineral studies. *Vib. Spectrosc.* **2003**, *31*, 1−10.

(9) Alizadehhesari, K.; Golding, S. D.; Bhatia, S. K. Kinetics of the dehydroxylation of serpentine. *Energy Fuels* **2012**, *26*, 783−790.

(10) Zhang, M.; Redfern, S. A. T.; Salje, E. K. H.; Carpenter, M. A.; Wang, L. H_2O and the dehydroxylation of phyllosilicates: An infrared spectroscopic study. *Am. Mineral.* **2010**, *95*, 1686−1693.

(11) Kristof, J.; Vassanyi, I.; Nemecz, E.; Inczedy, J. Study of the dehydroxylation of clay minerals using continuous selective water detector. *Thermochim. Acta* **1985**, *93*, 625−628.

(12) Meyers, S. T.; Anderson, J. T.; Hong, D.; Hung, C. M.; Wager, J. F.; Keszler, D. A. Solution-processed aluminum oxide phosphate thin-film dielectrics. *Chem. Mater.* **2007**, *19*, 4023−4029.

(13) Jiang, K.; Meyers, S. T.; Anderson, M. D.; Johnson, D. C.; Keszler, D. A. Functional ultrathin films and nanolaminates from aqueous solutions. *Chem. Mater.* **2013**, *25*, 210−214.

(14) Jiang, K.; Anderson, J. T.; Hoshino, K.; Li, D.; Wager, J. F.; Keszler, D. A. Low-energy path to dense HfO_2 thin films with aqueous precursor. *Chem. Mater.* **2011**, *23*, 945−952.

(15) Goncharova, L. V.; Dalponte, M.; Feng, T.; Gustafsson, T.; Garfunkel, E.; Lysaght, P. S.; Bersuker, G. Diffusion and interface growth in hafnium oxide and silicate ultrathin films on Si(001). *Phys. Rev. B* **2011**, *83*, No. 115329.

(16) Altamirano-Fortoul, R.; Le-Bail, A.; Chevallier, S.; Rosell, C. M. Effect of the amount of steam during baking on bread crust features and water diffusion. *J. Food Eng.* **2012**, *108*, 128−134.

(17) Le-bail, A.; Dessev, T.; Leray, D.; Lucas, T.; Mariani, S.; Mottollese, G.; Jury, V. Influence of the amount of steaming during baking on the kinetic of heating and on selected quality attributes of bread. *J. Food Eng.* **2011**, *105*, 379−385.

(18) Vanin, F. M.; Lucas, T. Crust formation and its role during bread baking. *Trends Food Sci. Technol.* **2009**, *20*, 333−343.

(19) Mondal, A.; Datta, A. K. Bread baking − A review. *J. Food Eng.* **2008**, *86*, 465−474.

(20) Banger, K. K.; Yamashita, Y.; Mori, K.; Peterson, R. L.; Leedham, T.; Rickard, J.; Sirringhaus, H. Low-temperature, high-performance solution-processed metal oxide thin-film transistors formed by a 'sol−gel on chip' process. *Nat. Mater.* **2011**, *10*, 45−50.

DOI: 10.1021/sc500824a
ACS Sustainable Chem. Eng. 2015, 3, 1081−1085